Journal of Materials Chemistry

Cite this: *J. Mater. Chem.*, 2011, **21**, 15327

www.rsc.org/materials

PAPER

Induction of supramolecular chirality in self-assembled nanofibers triggered by environmental change†

Zhegang Huang, Seong-Kyun Kang and Myongsoo Lee*

Received 11th June 2011, Accepted 4th August 2011
DOI: 10.1039/c1jm12683k

A carbazole end-capped rod amphiphile was synthesized and observed to self-assemble into non-chiral fibers in both methanol and water solutions even though the molecule contains a chiral oligoether dendron. Remarkably, a mixture of water and methanol induces supramolecular chirality of the nanofibers caused by a conformational change of hydrophobic aromatic rods and reduction in the hydrodynamic volume of the ethylene oxide chains. The helicity induction of the nanofibers also takes place by heating the water solution. Furthermore, the helical fibers in aqueous solution were observed to further aggregate into a rigid gel at higher temperature by enhanced hydrophobic interactions between the dehydrated oligo(ethylene oxide) dendrons.

Introduction

The construction of novel functional materials based on molecular self-assembly has received a great deal of attention in the fields of molecular and supramolecular materials.[1–3] Among the supramolecular nanostructures formed by the self-assembly of specifically designed molecules, a one-dimensional (1D) fibrillar assembly has proved to be particularly interesting for applications such as nanowires, gels, and biomimetic systems.[3] The 1D structure with stimulus-responsive features is likely to further enhance its scope to smart nanoscale materials. Although stimulus-responsive 1D nanostructures have been extensively studied, switching behavior triggered by external stimuli of the 1D fibrillar objects remains challenging.[4,5] Several years ago, we have shown that discrete cylindrical micelles can be interconnected by addition of a bridging agent to form reversible gels in aqueous solution.[6] We have also shown that T-shaped aromatic amphiphiles self-assemble into thermoresponsive nanofibers to form a 3D network gel upon heating.[7]

Center for Bio-responsive Assembly and Department of Chemistry, Seoul National University, Seoul, 151-747, Republic of Korea. E-mail: myongslee@snu.ac.kr; Fax: (+82) 2-393-6096

† Electronic supplementary information (ESI) available: DLS and TEM data of **1** in solutions and MODI-TOF MS of compound **1**. See DOI: 10.1039/c1jm12683k

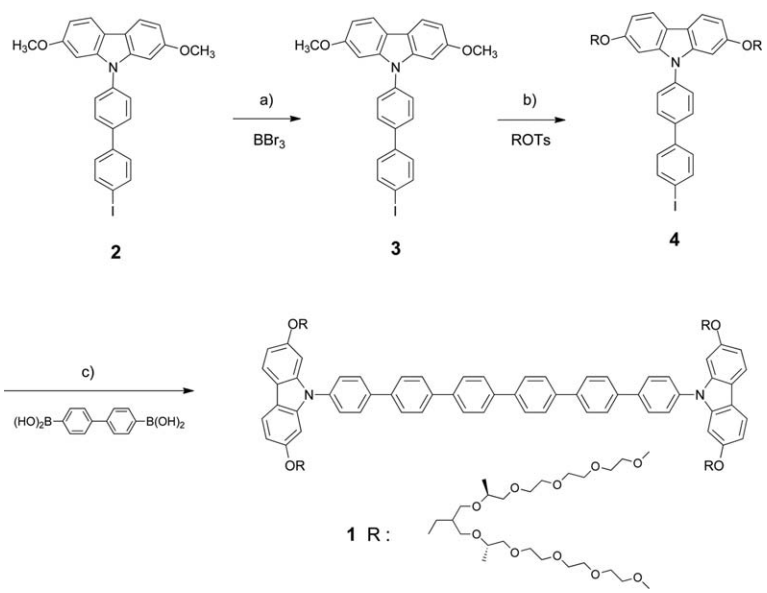

Scheme 1 Synthesis of the end-capped rod amphiphile **1**. (a) Dichloromethane; (b) K_2CO_3, acetonitrile, reflux; (c) Na_2CO_3, $[Pd(PPh_3)_4]$, THF, reflux.

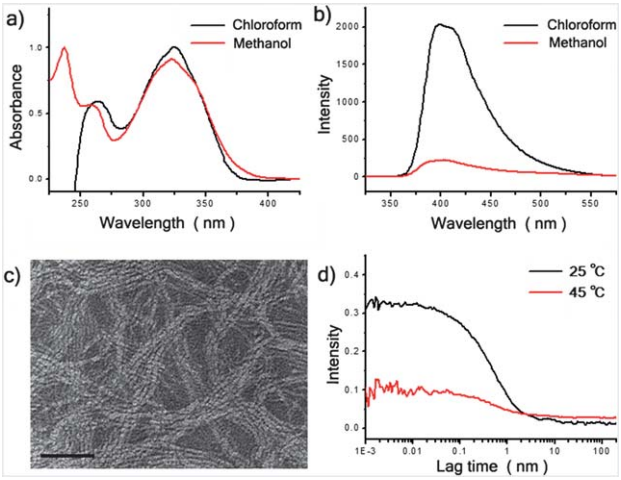

Fig. 1 (a) Absorption spectra of **1** in chloroform (2.0×10^{-5} M, black) and methanol (2.0×10^{-5} M, red). (b) Emission spectra of **1** in chloroform (2×10^{-5} M, black, $\lambda_{ex} = 320$ nm) and methanol (2×10^{-5} M, red, $\lambda_{ex} = 320$ nm). (c) TEM images of **1** methanol solution prepared at 25 °C (4×10^{-4} M, scale bars: 50 nm). (d) Autocorrelation functions of **1** in methanol (4×10^{-4} M) at 25 °C (black) and at 45 °C (red).

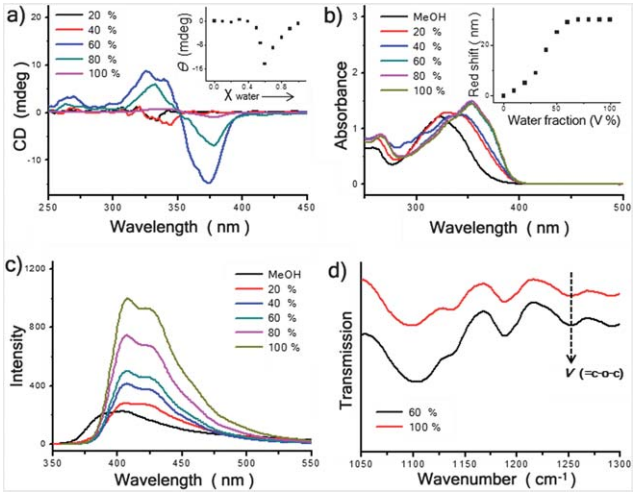

Fig. 2 (a) CD spectra of **1** in mixed solution with 10 mm cell (2×10^{-5} M); the inset shows the CD intensity variation at 378 nm with increasing molar fraction of water. (b) Absorption spectra of **1** in mixed solution (2.0×10^{-5} M); the inset shows the changes in the absorption maximum peak of **1**. (c) Emission spectra of **1** ($\lambda_{ex} = 320$ nm) in mixed solution (2×10^{-5} M). (d) FTIR spectra (1050–1300 cm^{-1}) of **1** in water–methanol mixed solution (water: 60%, black) and aqueous solution (red).

Recently, we have demonstrated that achiral nanofibers formed from a dumbbell-shaped rod amphiphile based on oligoether dendrons undergo a transition into chiral helical fibers triggered by lower critical solution temperature (LCST) of external oligoether chains in aqueous solution.[8] We envisioned that the amphiphilic molecules based on a conjugated rod can self-assemble into nanostructures even in polar organic solvents such as methanol, which is a selective solvent for oligoether dendrons.[9] With this idea in mind, we prepared amphiphile **1** containing a carbazole end-capped hexa-*p*-phenylene as an aromatic rod and oligo(ethylene oxide) dendrons according to previously reported similar methods and characterized by ^{1}H NMR spectroscopy and MALDI-TOF mass spectrometry (Scheme 1).[8,10] We present herein the formation of stimulus-responsive nanofibers from the self-assembly of rod amphiphiles. Notably, the self-assembled nanofibers respond to external stimuli such as temperature and solvent polarity by inducing supramolecular chirality.

Results and discussion

Molecule **1**, when dissolved in a solvent suitable for the oligoether dendron, can self-assemble into an aggregation structure due to its amphiphilic characteristics.[2a,11] Subsequently, the aggregation behavior of **1** in methanol was studied using UV/vis and fluorescence spectroscopy. The solution of **1** in chloroform (2.0×10^{-5} M) shows an absorption maximum at 325 nm (π–π^* transition) and emission maxima at $\lambda = 397$ and 410 nm (Fig. 1). Such spectra are similar to a general feature of 9-arylcarbazole derivatives revealing that there is a non-zero dihedral angle between the carbazole and the hexa-*p*-phenylene unit.[12] In contrast, the maximum of absorption in methanol is blue-shifted with respect to that observed in chloroform, and the fluorescence is significantly quenched, which is indicative of H-type interactions between the aromatic segments (Fig. 1).[13] Dynamic light scattering (DLS) experiments were performed with **1** in methanol solution (4.0×10^{-4} M) to further investigate the aggregation behavior. The CONTIN analysis of the autocorrelation function of **1** shows a broad peak that corresponds to a hydrodynamic radius (R_H) of ~100 nm.[14] To confirm the aggregation structures in methanol solution, TEM experiments were performed. As shown in Fig. 1c, the TEM image of **1** with a negatively stained sample shows one-dimensional cylindrical fibers with a uniform diameter of about 4.8 nm and lengths of several micrometres. By considering the extended molecular length (5.3 nm by CPK modeling), the image indicates that the diameter of the elementary cylindrical objects corresponds to one molecular length. This result suggests that molecule **1** self-assembles into cylindrical micelles consisting of solvophobic aromatic segments surrounded by solvophilic dendritic segments that are exposed to the methanol environment. Within the core, the rod segments stack on top of each other with mutual rotations to reduce steric repulsions between the twisted, non-planar aromatic rods. Notably, when molecule **1** in methanol solution was subjected to circular dichroism (CD) measurements, no CD signals could be detected even though **1** contains chiral side groups, indicating that the fibrillar objects are nonchiral. A temperature-dependent experiment reveals also no CD signal on heating and DLS shows that molecule **1** is molecularly dissolved over 45 °C (Fig. 1d). These results imply that the rod segments would be loosely packed with random stacks in methanol solution due to a non-planar aromatic conformation.

To investigate the influence of water on the methanol solution, the aggregation behavior of **1** was studied by addition of water into methanol solution (2×10^{-5} M). Remarkably, the CD spectra showed a strong positive and negative Cotton effect as the 60% water addition accompanied by notable changes in the absorption and emission spectra (Fig. 2a), indicating the helical stacks of the rod segments with a preferred handedness.[5] Upon

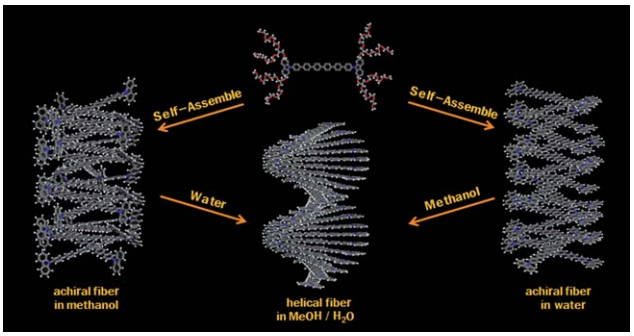

Fig. 3 Schematic representation of the reversible transformation from achiral to chiral states of the cylindrical stack in a mixture of methanol and water.

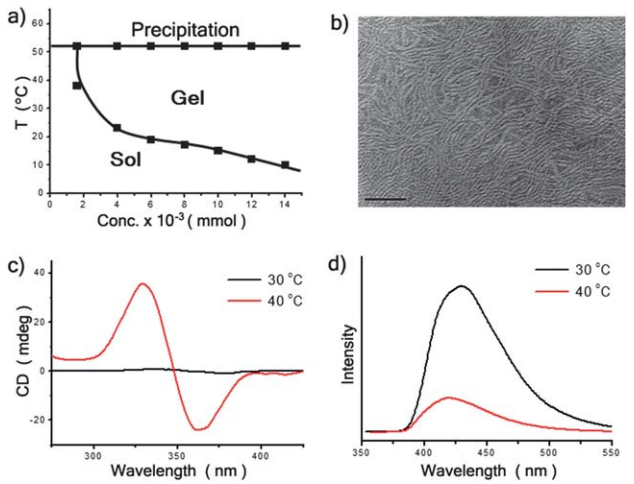

Fig. 4 (a) Phase diagram plotted in terms of the concentration of **1** *versus* temperature. (b) TEM images (negatively stained with uranyl acetate) of **1** in aqueous solution prepared at 40 °C (1.6×10^{-3} M, scale bars: 100 nm). (c) CD spectra of **1** in aqueous solution with 1 mm cell (1.6×10^{-3} M). (d) Emission spectra of **1** ($\lambda_{ex} = 340$ nm) in aqueous solution (1×10^{-3} M) at 30 °C (black) and 40 °C (red).

addition of water into methanol solution of **1**, the absorption maximum was red shifted and the intensity of emission was increased, indicating that the effective conjugation length of aromatic rod is extended due to the transition from twisted to planar conformations (Fig. 2b).[15] However, further addition of water results in a decrease in the intensity of the CD signal, which eventually disappeared in pure water. On the other hand, a gradual increase of the emission intensity was observed, suggesting the distance between the adjacent rods within the fibers increases due to increasing the effective volume fraction of oligoether dendrons caused by hydrogen bonding between ether oxygens and water molecules. The hydrated feature is reflected in FTIR spectroscopic experiments (Fig. 2d). The IR of **1** in mixed solution of methanol–water (2 : 3) showed two characteristic bands at 1250 cm^{-1} and 1105 cm^{-1} which correspond to phenyl ring-O and aliphatic C–O stretchings, respectively.[16] The band of 1105 cm^{-1} shifted to 1097 cm^{-1}, indicating that the oligoether chains are hydrated with addition of water through a hydrogen bonding interaction. This unique feature of induction of chirality can be explained by a conformational change of hydrophobic aromatic rods and variation in hydrodynamic volumes. Addition of water into the methanol solution would strengthen hydrophobic and π–π stacking interactions, which drives rod segments to be more planar for closer packing to result in steric constraints, giving rise to a helical arrangement. With further addition of water solvent, however, the oligoether chains would be fully hydrated to increase the effective volume fraction of oligoether chains. This increment would frustrate π–π stacking of aromatic rods which allow the rod segments to freely rotate within the aromatic core to block the chiral transfer from the side groups to the aromatic cores, thereby leading to non-chiral fibers (Fig. 3).

The nanofibers formed in aqueous solution would be entangled with each other above a LCST transition due to enhanced hydrophobic interactions.[7] In this context, we have measured viscosities with a capillary viscometer as a function of temperature. The solution viscosity of **1** (1.6×10^{-3} M) increases abruptly above 29 °C and results in gelation at 40 °C. The sol–gel transition temperature decreases to 10 °C with increasing concentration up to 1.4×10^{-2} M (Fig. 4a). The TEM image of the gel dried on a carbon-coated copper grid revealed the bundles of the nanofibers at higher temperatures, which demonstrates that the gel formation is attributed to the interconnection of the randomly oriented nanofibers (Fig. 4b). Interestingly, the CD spectra of **1** (1.6×10^{-3} M) showed a strong Cotton effect above the transition temperatures, indicating the formation of helical stacks of the rod segments with a preferred handedness (Fig. 4c).[5] Upon heating, the absorption spectra showed reduced intensity, and the fluorescence was quenched, indicating that the π–π stacking interactions between the aromatic rods are enhanced (Fig. 4d).[14,17] These results suggest that the helicity induction of the nanofibers upon heating arises from closer packing between the adjacent aromatic units within the core, and the helical fibers were further aggregated into a rigid gel above a certain concentration. This thermoresponsive solution behavior can be explained by considering the entropically driven dehydration of the oligoether chains, as the solution is heated.[18] With increasing temperature, the ethylene oxide chains would be dehydrated that drives the fibers with more hydrophobic surfaces, thus resulting in enhanced hydrophobic interactions between the adjacent fibrils to form 3D networks. This enhanced hydrophobic environment also leads to a decrement of the aromatic stacking distance with restricted rotational freedom, thus the helical stacks are formed through steric constraints of the aromatic segments.[8]

Conclusions

The results described here demonstrated that a carbazole end-capped aromatic amphiphile self-assembles into stimulus-responsive fibers. In a pure solution of methanol or water, the molecule was observed to self-assemble into non-chiral fibers consisting of aromatic cores surrounded by hydrophilic oligo (ethylene oxide) dendritic segments. Notably, these nanofibers were shown to recognize temperature or solvent polarity changes by inducing supramolecular chirality. Upon mixing water and methanol solutions of **1**, the achiral nanofibers transform into 1D objects with supramolecular chirality due to both packing constraints and a conformational change of the rod segments.

The helicity induction of the nanofibers also takes place by heating the aqueous solution. Upon heating, the ethylene oxide chains would be dehydrated, which results in enhanced π–π stacking interaction to force the aromatic rods to be arranged with helical stacking. Another interesting point to be noted is that the nanofibers are interconnected to form thermo-responsive gels through enhanced hydrophobic interactions.

Experimental

Materials

NaH (60%) and *p*-toluenesulfonyl chloride (98%) from Tokyo Kasei were used as received. 4,4′-Diiodobiphenyl (98%) from Lancaster was used as received. Unless otherwise indicated, all starting materials were obtained from Aldrich and were used without purification. Dry THF was obtained by vacuum transfer from sodium and benzophenone. Compounds were synthesized according to the procedure described in Scheme 1, and the starting materials **2** and oligo-ethylene oxide segments were synthesized using a similar procedure described previously.[8,10]

Techniques

^{1}H NMR spectra were recorded from $CDCl_3$ or DMSO solutions on a Bruker AM 250 spectrometer. Dynamic light scattering (DLS) measurements were performed using a DLS-8000 from Otsuka Electronics with a 632.8 nm He–Ne laser. UV/vis absorption spectra were obtained from a Hitachi U-2900 Spectrophotometer. The fluorescence spectra were obtained from a Hitachi F-7000 Fluorescence Spectrophotometer. Circular dichroism (CD) spectra were obtained using a JASCO J-810 spectropolarimeter. Transmission electron microscopy (TEM) was performed at 120 kV using a JEOL-JEM 2100. MALDI-TOF-MS was performed on a Bruker Microflex LRF20 using α-cyano-4-hydroxy cinnamic acid (CHCA) as matrix. Preparative high performance liquid chromatography (HPLC) was performed at room temperature using a 20 mm × 600 mm polystyrene column on a Japan Analytical Industry Model LC-908 recycling preparative HPLC system, equipped with a UV detector 310 and a RI detector RI-5.

Synthesis

Synthesis of compound 3. BBr_3 (15 ml, 15 mmol) was dropped into a solution of compound **2** (1.24 g, 2.45 mmol) in methylene chloride 40 mL slowly at 0 °C. The reaction mixture was stirred at room temperature under nitrogen for 6 h. The solution was quenched with MeOH for 30 min. Then the resulting solution was washed with water and the methylene chloride solution, dried over anhydrous magnesium sulfate, and filtered. The solvent was removed in a rotary evaporator, and the crude product was purified by column chromatography (silica gel) using ethyl acetate : hexane (2 : 3 v/v) to yield 1.1 g (94%) of a white powder. ^{1}H NMR (250 MHz, DMSO, δ, ppm) 9.36 (s, 2H, ArOH), 7.89 (m, 6Ar–H), 7.6 (m, 4Ar–H), 6.69 (m, 4 Ar–H).

Synthesis of compound 4. Compound **3** (0.23 g, 0.47 mmol), ROTs (0.72 g, 1.08 mmol) and excess K_2CO_3 were dissolved in 30 ml of anhydrous acetonitrile. The mixture was refluxed for 24 h. The resulting solution was poured into water and extracted with methylene chloride. The methylene chloride solution was washed with water, dried over anhydrous magnesium sulfate, and filtered. The solvent was removed in a rotary evaporator, and the crude product was purified by column chromatography (silica gel) using ethyl acetate/methanol (20 : 1 v/v) to yield 0.58 g (68%) of a waxy solid. ^{1}H NMR (250 MHz, $CDCl_3$, δ, ppm) 7.87 (d, 2Ar–H, *o* to I, 8.8 Hz), 7.77 (m, 4Ar–H), 7.59 (d, 2Ar–H, *m* to OCH2, 8.5 Hz), 7.44 (d, 2Ar–H, *m* to I, 8.8 Hz), 6.85 (m, 4Ar–H), 4.11 (d, 4H, 2 × CH_2Ophenyl, J = 3.5 Hz), 3.82–3.51 (m, 68H, OCH_2), 3.37 (s, 12H, OCH_3), 2.2–2.5 (m, 2H, 2 × $CH(CH_2)_3$), 1.06–1.17 (m, 12H, 4 × CHCH_3).

Synthesis of compound 1. Compound **4** (0.36 g, 0.239 mmol) and 4,4′-biphenyl diboronic acid (28.8 mg, 0.12 mmol) were dissolved in degassed THF (25 ml). Degassed 2 M aqueous Na_2CO_3 (25 ml) was added to the solution and then tetrakis (triphenylphosphine) palladium(0) (5 mg, 0.004 mmol) was added. The mixture was refluxed for 24 h with vigorous stirring under nitrogen. Cooled to room temperature, the layers were separated, and the aqueous layer was then washed twice with methylene chloride. The combined organic layer was dried over anhydrous magnesium sulfate and filtered. The solvent was removed in a rotary evaporator, and the crude product was purified by column chromatography (silica gel) using ethyl acetate/methanol (10 : 1 v/v) as eluent and by prep. HPLC to yield 0.14 g (40%) of a waxy solid. ^{1}H NMR (250 MHz, $CDCl_3$, δ, ppm) 7.93–7.81 (m, 24Ar–H), 7.65 (d, 4Ar–H, *m* to OCH_2, 8.5 Hz), 6.86 (m, 8Ar–H), 4.06 (d, 8H, 4 × CH_2Ophenyl, J = 4.8 Hz), 3.64–3.49 (m, 136H, OCH_2), 3.36 (m, 24H, OCH_3), 2.37–2.31 (m, 4H, phenyl$OCH_2CH(CH_2O)_2$), 1.13–1.08 (m, 24H, 8 × CHCH_3): ^{13}C NMR (60 MHz, $CDCl_3$, ppm): = 157.9, 142.2, 139.9, 139.8, 139.6, 137.0, 128.7, 127.7, 127.6, 119.0, 117.2, 95.2, 71.7, 70.8, 70.5, 69.7, 69.4, 66.5, 59.1, 40.2, 17.43, 17.30; Anal. Calcd for $C_{156}H_{232}N_2O_{44}$: C, 65.99; H, 8.24; N, 0.99. Found C, 65.65; H, 8.32; N, 1.03%. MALDI-TOF-MS *m*/*z* $(M + H)^+$ 2840.5, $(M + Na)^+$ 2862.8.

Acknowledgements

This work was supported by the National Research Foundation of Korea (NRF) grant funded by the Korean government (MEST) (2011-0018311) and U.S. Air force Office of Scientific Research (FA 2386-10-1-4087). We acknowledge a fellowship of the BK21 program from the Ministry of Education and Human Resources Development.

Notes and references

1 (*a*) F. J. M. Hoeben, P. Jonkheijm, E. W. Meijer and A. P. H. J. Schenning, *Chem. Rev.*, 2005, **105**, 1491; (*b*) J. J. L. M. Cornelissen, A. E. Rowan, R. J. M. Nolte and N. A. J. M. Sommerdijk, *Chem. Rev.*, 2001, **101**, 4039; (*c*) M. Enomoto, A. Kishimura and T. Aida, *J. Am. Chem. Soc.*, 2001, **123**, 5608; (*d*) S. Kawano, N. Fujita and S. Shinkai, *J. Am. Chem. Soc.*, 2004, **126**, 8592.
2 (*a*) H.-J. Kim, Y.-b. Lim and M. Lee, *J. Polym. Sci., Part A: Polym. Chem.*, 2008, **46**, 1925; (*b*) V. Percec, J. G. Rudick, M. Peterca and P. A. Heiney, *J. Am. Chem. Soc.*, 2008, **130**, 7503; (*c*) A. Khan, C. Kaiser and S. Hecht, *Angew. Chem., Int. Ed.*, 2006, **45**, 1878; (*d*) M. T. Stone and J. S. Moore, *J. Am. Chem. Soc.*, 2005, **127**, 5928.

3 (*a*) L. C. Palmer and S. I. Stupp, *Acc. Chem. Res.*, 2008, **41**, 1674; (*b*) J. P. Hill, W. Jin, A. Kosaka, T. Fukushima, H. Ichihara, T. Shimomura, K. Ito, T. Hashizume, N. Ishii and T. Aida, *Science*, 2004, **304**, 1481.
4 (*a*) J. Rodriguez-Hernandez and S. Lecommandoux, *J. Am. Chem. Soc.*, 2005, **127**, 2026; (*b*) Z. Hu, A. M. Jonas, S. K. Varshney and J.-F. Gohy, *J. Am. Chem. Soc.*, 2005, **127**, 6526; (*c*) J. Xu and E. R. Zubarev, *Angew. Chem., Int. Ed.*, 2004, **43**, 5491; (*d*) K. Kuroiwa, T. Shibata, A. Takada, N. Nemoto and N. Kimizuka, *J. Am. Chem. Soc.*, 2004, **126**, 2016.
5 (*a*) H. Engelkamp, S. Middelbeek and R. J. M. Nolte, *Science*, 1999, **284**, 785; (*b*) P. Jonkheijm, P. V. D. Schoot, A. P. H. J. Schenning and E. W. Meijer, *Science*, 2006, **313**, 80.
6 J.-H. Ryu and M. Lee, *J. Am. Chem. Soc.*, 2005, **127**, 14170.
7 K.-S. Moon, H.-J. Kim, E. Lee and M. Lee, *Angew. Chem., Int. Ed.*, 2007, **46**, 6807.
8 Z. Huang, E. Lee, H.-J. Kim and M. Lee, *Chem. Commun.*, 2009, 6819.
9 (*a*) E. Lee, Z. Huang, J.-H. Ryu and M. Lee, *Chem.–Eur. J.*, 2008, **14**, 6957; (*b*) P. Zhou and W. Brown, *Macromolecules*, 1990, **23**, 1131.
10 H.-J. Kim, W.-C. Zin and M. Lee, *J. Am. Chem. Soc.*, 2004, **126**, 7009.
11 J.-H. Ryu, D.-J. Hong and M. Lee, *Chem. Commun.*, 2008, 1043.
12 M. M. Palau, E. Perea, F. L. Calahorra and D. Velasco, *Lett. Org. Chem.*, 2004, **1**, 231.
13 (*a*) P. A. van Hal, M. M. Weink, J. M. Kroon and R. A. J. Janssen, *J. Mater. Chem.*, 2003, **13**, 1054; (*b*) T. Mori, T. Watanabe, K. Minagawa and M. Tanaka, *J. Polym. Sci., Part A: Polym. Chem.*, 2005, **43**, 1569.
14 See the ESI†.
15 B.-K. An, S.-K. Kwon, S.-D. Jung and S.-Y. Park, *J. Am. Chem. Soc.*, 2002, **124**, 14410.
16 W. Li, S. Y. Yin, Y. Q. Wu and L. X. Wu, *J. Phys. Chem. B*, 2006, **110**, 16961.
17 (*a*) R. W. Sinkeldam, F. J. M. Hoeben, M. J. Pouderoijen, I. De Cat, J. Zhang, S. Furukawa, S. De Feyter, J. A. J. M. Vekemans and E. W. Meijer, *J. Am. Chem. Soc.*, 2006, **128**, 16113; (*b*) T. Nakano and T. Yade, *J. Am. Chem. Soc.*, 2003, **125**, 15474.
18 (*a*) G. D. Smith and D. Bedrov, *J. Phys. Chem. B*, 2003, **107**, 3095; (*b*) B. Jeong, Y. H. Bae and S. W. Kim, *Macromolecules*, 1999, **32**, 7064.